Real-Time, Multiday Cell Stress Assay

Quantifying the unfolded protein response using a nontoxic genetically encoded fluorescent sensor, live-cell imaging, and label-free cellular impedance

Authors

Nancy Li, Yama Abassi,
Xiaobo Wang, David Ferrick,
and Brandon J. Lamarche
Agilent Technologies, Inc.

Introduction

Moving beyond the mere "snapshots" that are provided by traditional endpoint assays, live-cell imaging makes it possible to observe the full continuum of biological processes such as proliferation, killing, activation, differentiation, etc. While brightfield images serve as the foundation of these assays, the inclusion of nontoxic exogenous fluorescent probes facilitates quantification of general characteristics such as the exact number of cells present, or of specific characteristics such as the progression of apoptosis. Designing live-cell-compatible fluorescent probes that provide multiday, real-time information about a specific biochemical pathway is not trivial, as they must fluoresce in a manner that reflects the pathway's status, localize to the appropriate cellular compartment, and be stable, noncytotoxic, nonperturbing, and appropriately soluble. As an alternative to the use of exogenous probes, the cells themselves can be endowed with a genetically encoded fluorescent sensor that provides continuous feedback regarding specific biochemical phenomena. This application note demonstrates such an approach, coupling the Agilent xCELLigence RTCA eSight live-cell imager with a genetically encoded dual-color fluorescent sensor of a key stress pathway, the unfolded protein response (UPR). With minimal hands-on time and high-throughput capacity, the assay conditions are optimized quickly and with ease. Subsequently, drug-mediated stimulation of the UPR is shown to induce expression of the fluorescent sensor protein in a time- and dose-dependent manner, and with an EC_{50} value that is essentially identical to literature-reported values. Concordant with image acquisition, eSight's label-free, real-time tracking of cellular impedance, which interrogates cell number/size/attachment strength/barrier function, provides confirmatory results from an orthogonal perspective. Coupling of the image-based and impedance-based kinetic readouts yields a deeper understanding of the cells' health and behavior throughout the full continuum of the UPR, and lends itself to in-depth mechanistic analyses. The principles demonstrated herein are not confined to the UPR; they are broadly applicable to real-time eSight assays employing genetically encoded fluorescent sensors in general.

Genetically encoded UPR sensor

Proteins destined for the secretory pathway are translated by ribosomes that are bound to the outer surface of the endoplasmic reticulum (ER). As they emerge from the ribosome these nascent polypeptides protrude into the ER lumen where they undergo: N-linked glycosylation, disulfide bond formation, and folding. Overwhelming this system can lead to the accumulation of unfolded/misfolded proteins within the ER lumen, which in turn triggers a stress pathway called the unfolded protein response (UPR).[1] UPR activation orchestrates the recovery of ER function by, in part, increasing the concentration of protein folding chaperones in the ER lumen. In situations where ER stress is irreversible, the UPR triggers apoptosis.[1]

Three different UPR sensors have been identified, each of which span the ER membrane and transduce stress signals from the lumen into the cytoplasm, with the signal ultimately cascading into the nucleus where it impacts gene expression.[2] ER stress causes one of these sensors, IRE1, to dimerize, which in turn activates its cytoplasmic endoribonuclease domain (Figure 1). This nuclease domain of IRE1 excises an intron from the mRNA of the transcription factor XBP1. This leads to the production of a stabilized form of the XBP1 protein which translocates to the nucleus and upregulates the expression of diverse proteins that help mitigate ER stress[2] (Figure 1).
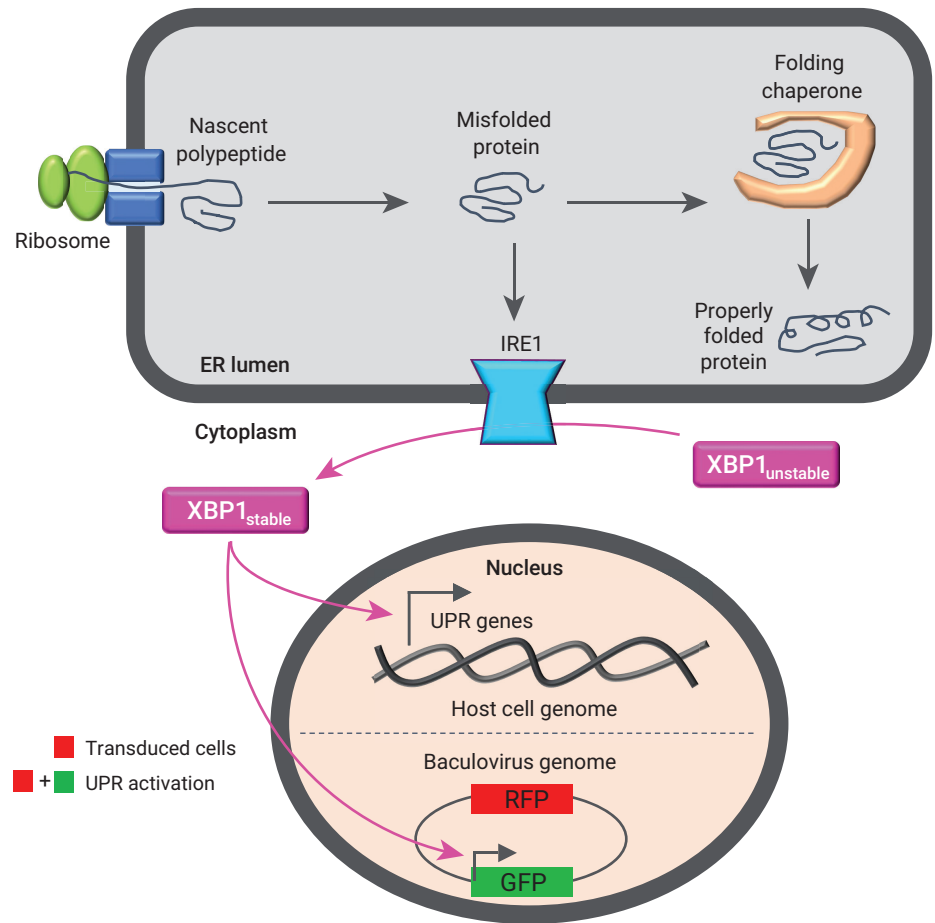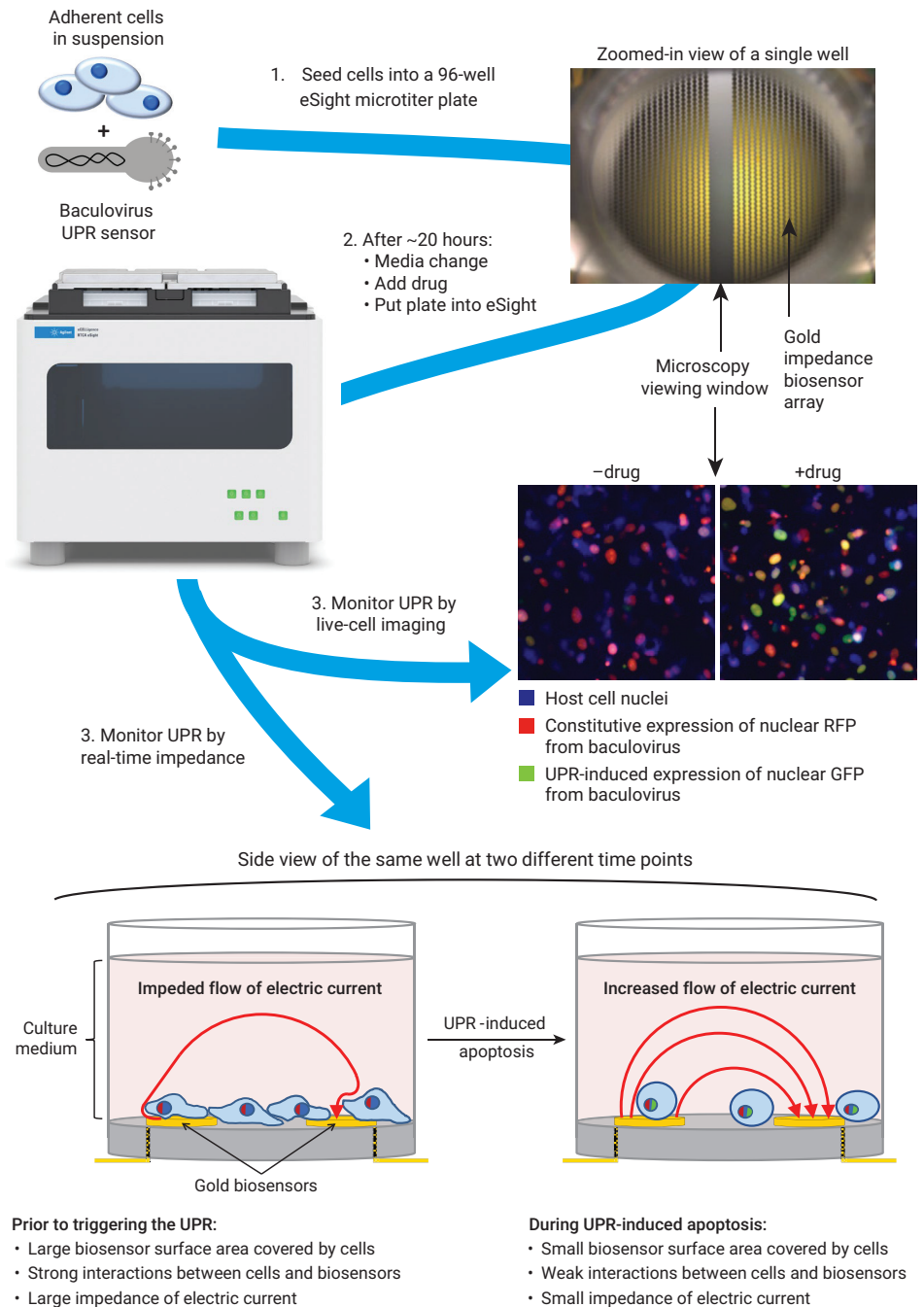

Figure 1. Genetically encoded fluorescent sensor for monitoring the UPR in real time. Rather than depicting in detail its role in XBP1 mRNA splicing, here IRE1 is simply shown to be responsible for generating a stable form of the XBP1 protein which can translocate to the nucleus. While cells containing the baculovirus UPR sensor are constitutively red, those in which the UPR has been activated are both red and green. See text for a full description.

The Green/Red Fluorescent Cell Stress sensor from Montana Molecular is a baculovirus that encodes: i) nuclear-localized red fluorescent protein (RFP) that is expressed constitutively, and ii) nuclear-localized green fluorescent protein (GFP) that is only expressed in the presence of stabilized XBP1. While the RFP signal indicates which cells contain the baculovirus, the GFP signal serves as a sensor of UPR activation (Figure 1).

eSight assay principle

The eSight is currently the only instrument that interrogates cell health and behavior using cellular impedance and live-cell imaging simultaneously. When using eSight's specialized microplates, which contain gold biosensor arrays integrated into the bottom of all 96 wells (Figure 2), real-time impedance measurements track changes in cell number, cell size, cell-substrate attachment strength, and cell-cell interactions (i.e. barrier function). Positioned in between the gold biosensors, a microscopy viewing window enables eSight to concurrently collect live-cell images that include brightfield as well as red, green, and blue fluorescence (Figure 2). This ability to monitor an assay in real time from two orthogonal perspectives, using the same population of cells, provides a richer data output (both primary and confirmatory results) all from a single simple assay.

Adherent cells in suspension

+

Baculovirus UPR sensor

1. Seed cells into a 96-well eSight microtiter plate

2. After ~20 hours:
   • Media change
   • Add drug
   • Put plate into eSight

Zoomed-in view of a single well

Microscopy viewing window

Gold impedance biosensor array

−drug   +drug

3. Monitor UPR by live-cell imaging

3. Monitor UPR by real-time impedance

■ Host cell nuclei
■ Constitutive expression of nuclear RFP from baculovirus
■ UPR-induced expression of nuclear GFP from baculovirus

Side view of the same well at two different time points

Impeded flow of electric current

Culture medium

Gold biosensors

UPR-induced apoptosis

Increased flow of electric current

Prior to triggering the UPR:
• Large biosensor surface area covered by cells
• Strong interactions between cells and biosensors
• Large impedance of electric current

During UPR-induced apoptosis:
• Small biosensor surface area covered by cells
• Weak interactions between cells and biosensors
• Small impedance of electric current

Figure 2. Agilent xCELLigence RTCA eSight live-cell imager workflow for real-time UPR assays. Changes in the fluorescent properties of the cells' nuclei upon UPR activation are described in the text.

Materials and methods

Cell maintenance and assays were conducted at 37 °C/5% CO_2 in EMEM media (ATCC; part number 30-2003) containing 10% heat inactivated FBS (Corning, part number 35016CV). The HT-1080-Blue cell line, which stably expresses nuclear-localized blue fluorescent protein (BFP), was produced by transducing HT-1080 cells (ATCC; part number CCL-121) with Agilent eLenti Blue (part number 8711012) at a multiplicity of infection of 1. From day 2 to day 11 postinfection, 1 µg/mL puromycin was included in the growth medium to select for transductants. The baculovirus Green/Red Fluorescent Ratiometric Cell Stress Sensor (i.e. UPR sensor), thapsigargin, and sodium butyrate were supplied in a kit from Montana Molecular (part number U0901G). E-Plate VIEW microplates were from Agilent Technologies (part number 00300601030).

To optimize assay conditions, 25 µL of media was added to wells of an E-Plate VIEW. After briefly spinning the plate to ensure media coverage of the entire well bottom, the background impedance was measured. Subsequently, each well received 125 µL of a solution containing cells (12.5, 25, or 50 k), baculovirus UPR sensor (5, 10, 20, or 40 µL), and sodium butyrate (0, 1, 2, or 4 mM). After allowing the cells to settle for 30 minutes at room temperature, plates were transferred to the eSight inside an incubator and data acquisition was initiated.

For characterizing drug-mediated induction of the UPR the protocol was similar to that described above, but transduction conditions were fixed at 10 k cells/well, 20 µL of baculovirus UPR sensor/well, and 2.4 mM sodium butyrate. 21.5 hours after seeding the cells the entire 150 µL of transfection mixture/media was aspirated from each well and replaced with 100 µL of EMEM containing 10% FBS and 2 mM sodium butyrate. Cells were allowed to recover for 12 hours and then each well received an additional 100 µL of EMEM containing 10% FBS, 2 mM sodium butyrate, and varying concentrations of thapsigargin.

For all eSight assays impedance was measured every 15 minutes, while images were acquired once per hour. In each well, four fields of view were captured for each channel (brightfield, red, green, and blue). Exposure times were as follows: brightfield (automatically adjusted by the eSight software), red (500 ms), green (300 ms), and blue (80 ms).

Results and discussion

Optimizing baculovirus transduction and transgene expression

Prior to assaying UPR activation, the baculovirus must be transduced into host cells under conditions which allow for its genome to remain transcriptionally active. As part of their intrinsic immune resonse mammalian cells can bind up the baculovirus genome with histones and thereby suppress transgene expression.[3] Inclusion of butyrate in the transduction medium can block this process by inhibiting histone deacetylase[4], allowing the baculovirus genome to properly express RFP constitutively, and to express GFP when the UPR is activated.
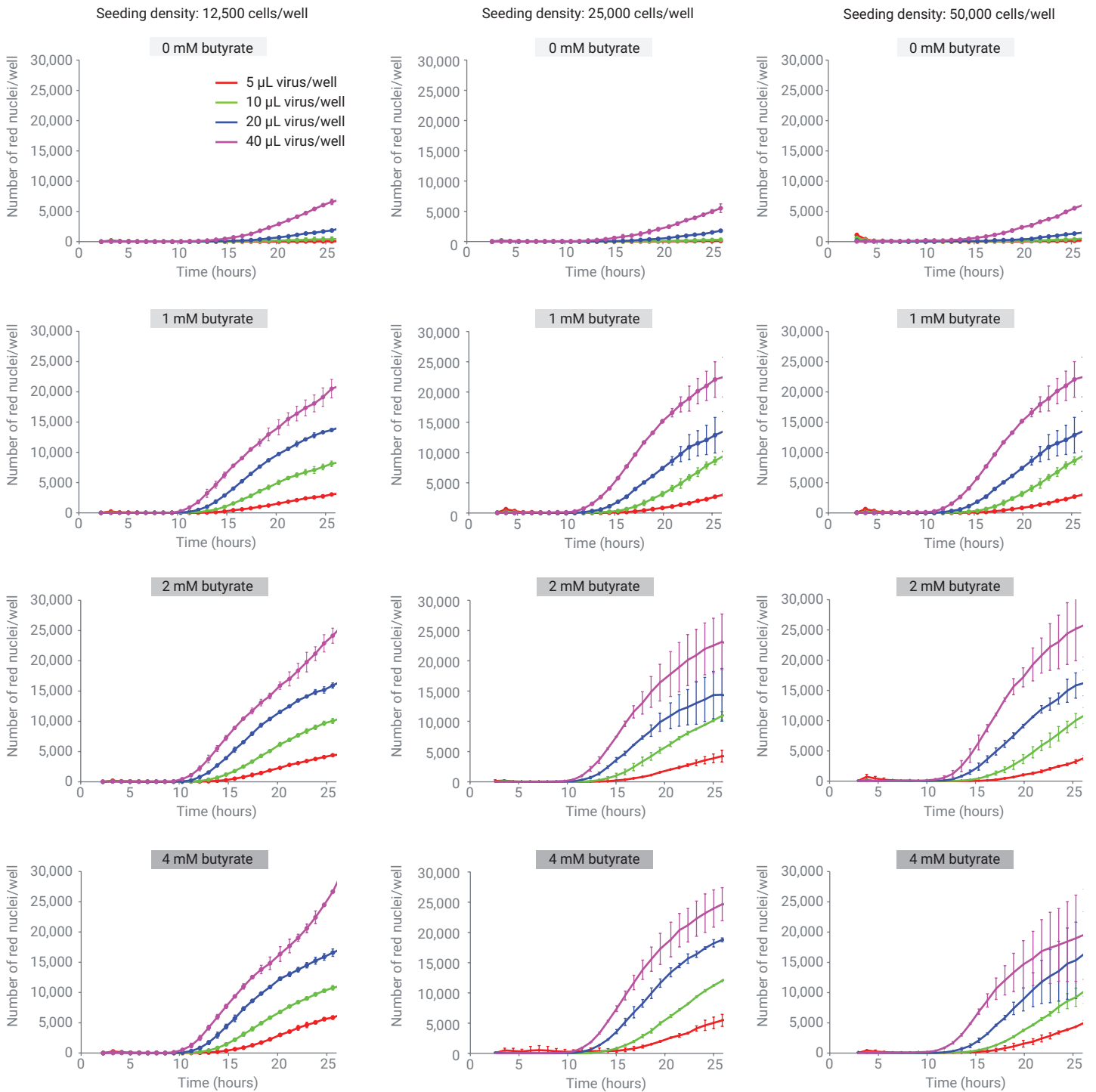
As a first step towards evaluating baculovirus transduction efficiency and the extent to which the baculovirus genome remains transcriptionally accessible within the host cell nucleus, HT-1080-Blue cells (12,500/well) were transduced with 20 or 40 µL/well of the baculovirus in the presence of either 0 or 4 mM butyrate. Figure 3 clearly demonstrates that in the absence of butyrate the baculovirus genome is transcriptionally suppressed (i.e. very few cells express RFP, which is supposed to be expressed constitutively, irregardless of UPR activation). However, inclusion of 4 mM butyrate enables RFP to be expressed earlier, in greater abundance per cell, and in a greater percentage of the cells (Figure 3). To more exhaustively optimize baculovirus transduction and the accessibility of its transgenes for transcription, the number of target cells was varied (12.5, 25, or 50 k/well) while simultaneously varying the amount of virus (5, 10, 20, or 40 µL/well) and the butyrate concentration (0, 1, 2, or 4 mM). These data, plotted as the number of red nuclei/well as a function of time post transduction, are summarized in Figure 4 and provide four important conclusions. First, as expected the number of cells displaying the RFP signal is always proportional to the quantity of virus used per well. Second, while transitioning from 0 to 1 mM butyrate provides substantial gains in the number of cells that are RFP-positive, increasing the concentration up to 2 or 4 mM provides diminishing returns. Third, RFP is not detectable until at least 10 hours post transduction, but then increases steadily over the next 15 hours. Fourth, the number of RFP expressing cells does not vary dramatically as a function of target cell seeding density.

Visual inspection of cells across the different transduction conditions showed that wells which were seeded with 25 or 50 k cells were already confluent when RFP expression first became detectable (data not shown). Also, cells exposed to 40 µL virus/well displayed a substantial cytopathic effect (data not shown). On the basis of these findings, it was determined that: i) the cell seeding density should be ≤12.5k/well (to ensure that cells are still proliferating when UPR activation is being interrogated), and ii) the quantity of virus should be ≤20 µL/well.
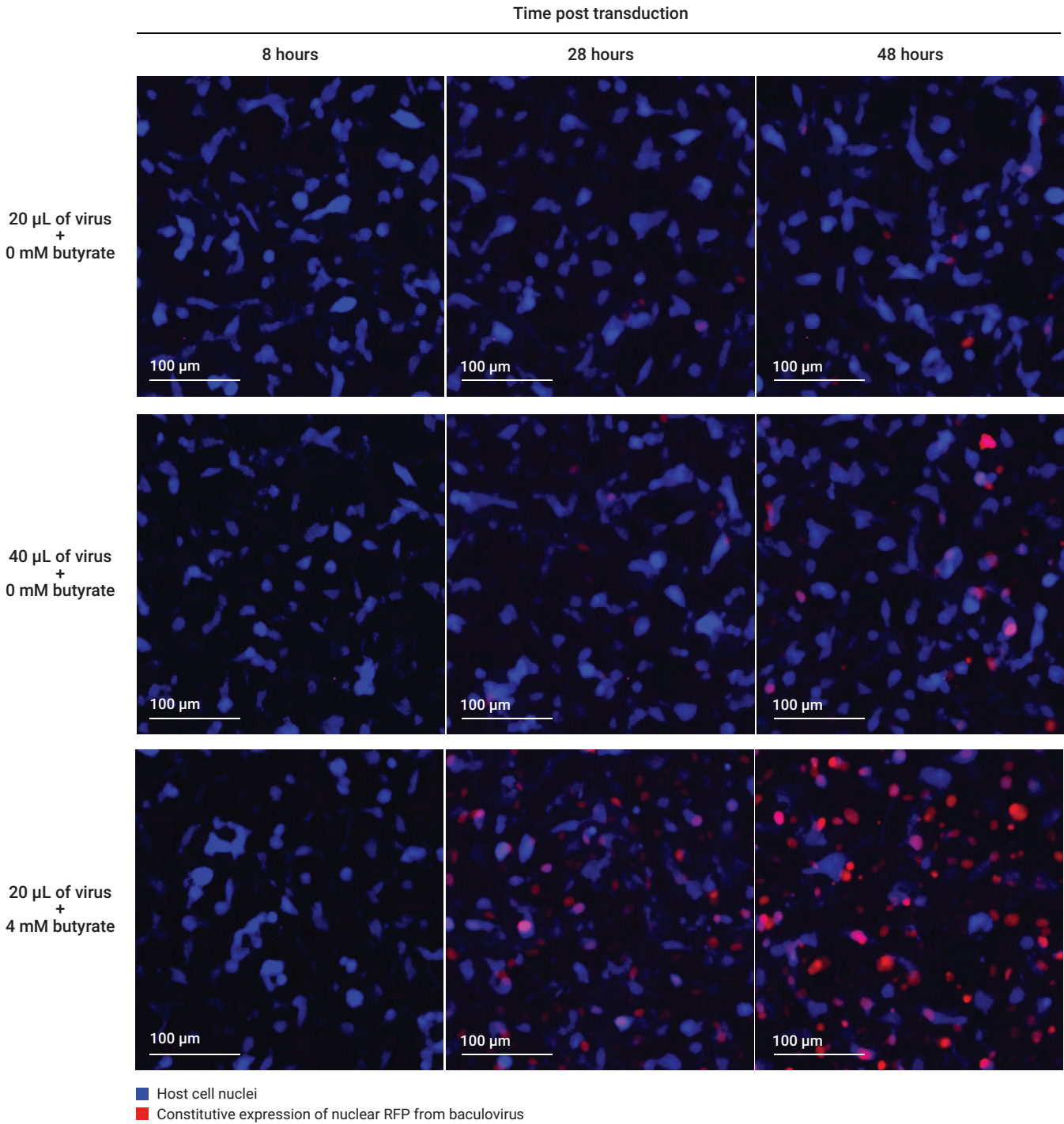
Figure 3. Butyrate prevents the host cell from blocking transgene expression from the baculovirus genome. Expression of the baculovirus-encoded RFP is driven by a constitutive promoter. Consequently, the extent to which the baculovirus genome remains transcriptionally accessible within the host cell nucleus can be evaluated based on the percentage of cells that are RFP-positive, and/or the brightness of the RFP signal in each cell.

Figure 4. Real-time screening of multiple parameters that impact baculovirus transduction efficiency and the extent to which the baculovirus genome remains transcriptionally accessible within the host cell nucleus. See text for details.

Focusing on the 12.5k cells/well condition, a systematic comparison of the different virus and butyrate combinations was undertaken. As an alternative means of representing the same data from Figure 4, Figure 5 plots the % transduction [(no. of red cells per well/no. of blue cells/well) × 100]. Note that upon progressing from 24 to 36 to 48 hours post transduction, the percentage of red cells increases for all combinations examined. Importantly, however, at 20 μL virus + 4 mM butyrate the % transduction actually appears to exceed 100% at the 36 and 48 hour time points. Visual inspection of the cells immediately provides an explanation for this aberrant behavior. In contrast to the lower butyrate concentrations, cells exposed to 4 mM butyrate display substantial cytotoxicity (Figure 6). Robust RFP expression combined with the fragmentation of these cells makes it appear that the number of transduced cells (red) exceeds the total number of cells (blue) in the well.
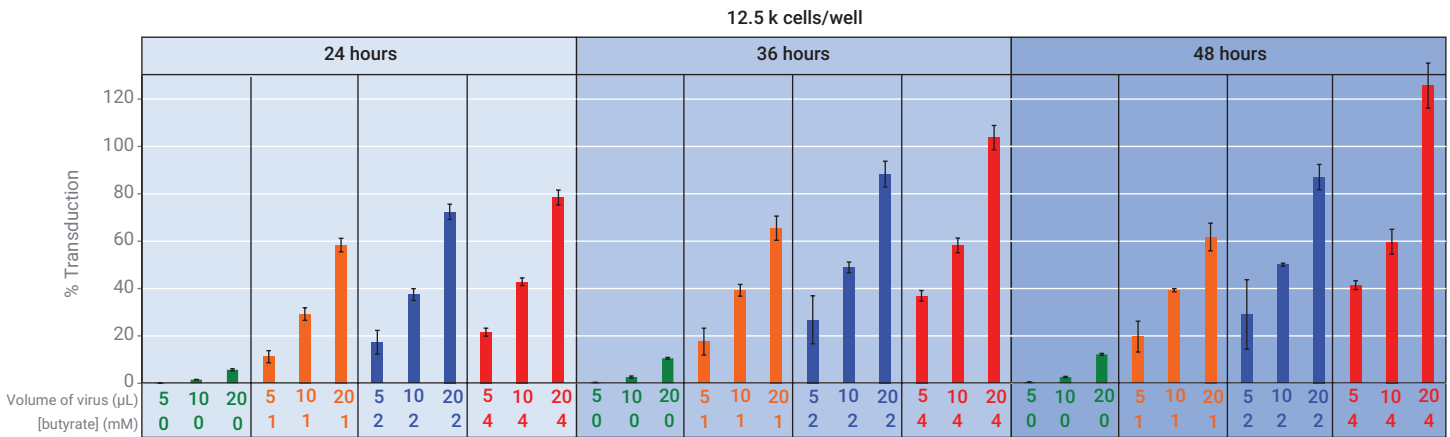

Figure 5. Summary of transduction efficiency, for different virus and butyrate combinations, when using 12,500 cells/well.
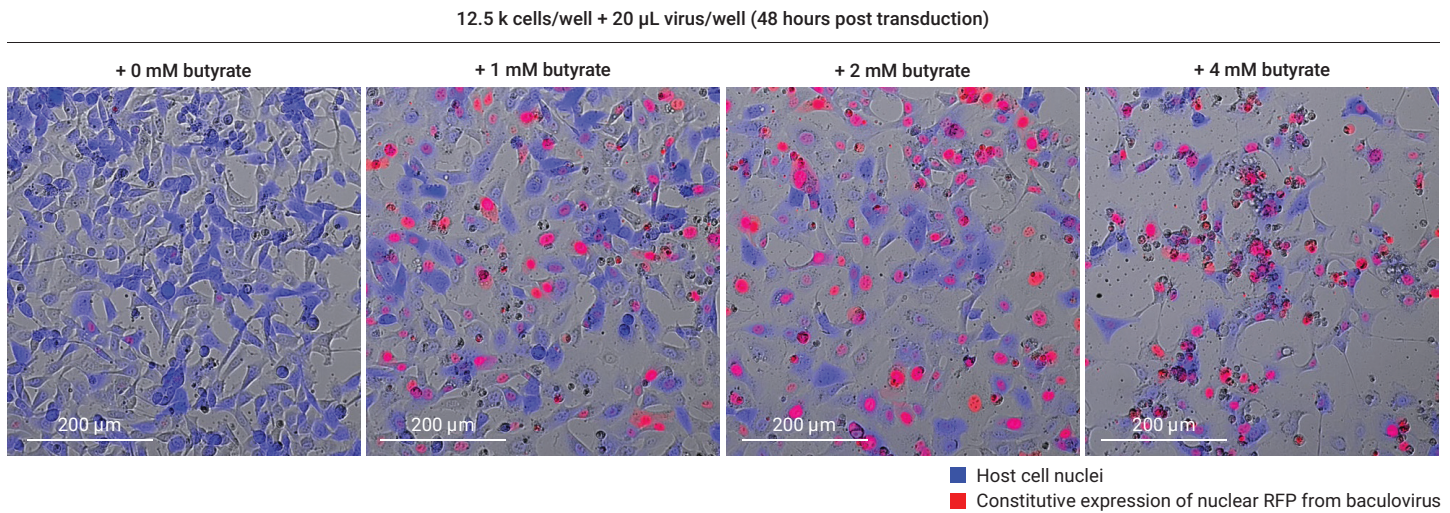

Figure 6. Although butyrate improves baculovirus transgene expression, it becomes toxic at higher concentrations.

Tracking UPR activation in real time

Based on the entirety of the above data, transduction conditions were finalized as 10 k HT-1080-Blue cells, 20 µL virus, and 2.4 mM butyrate. 21.5 hours after seeding, the transfection mixture was aspirated and replaced with media containing 2 mM butyrate. Cells were allowed to recover for 12 hours and then each well was supplemented with varying concentrations of the drug thapsigargin, which blocks transport of Ca^{2+} into the ER[5] and thereby activates the UPR[6]. As shown in Figure 7, even in the absence of thapsigargin, a modest amount of GFP is detectable. Whether this is due to a bona fide background level of UPR activation versus just leaky/nonspecific expression from the UPR sensor was not investigated. Importantly, the inclusion of thapsigargin dramatically stimulates GFP expression – with the number of GFP-positive cells and the average GFP signal/cell both increasing. Plotting the total integrated intensity* of the GFP signal as a function of time reveals a clear dose dependency for thapsigargin induction of the UPR.

* Total integrated intensity is a summation of all green light emitted from the well bottom. It therefore takes into account both changes in the number of cells that express GFP as well as the amount of GFP per cell.

Figures 8A and 8B display this data with and without the standard deviation, respectively. In addition to the magnitude of the GFP signal varying as a function of thapsigargin concentration, the time at which the GFP signal peaks is also dose dependent (Figure 8B): the higher the drug concentration, the more rapidly the GFP signal peaks. This is consistent with a "threshold effect", where low concentrations of thapsigargin are still sufficient for disrupting calcium homeostasis in the ER, but it takes longer for this to reach a crisis point where the UPR is activated.
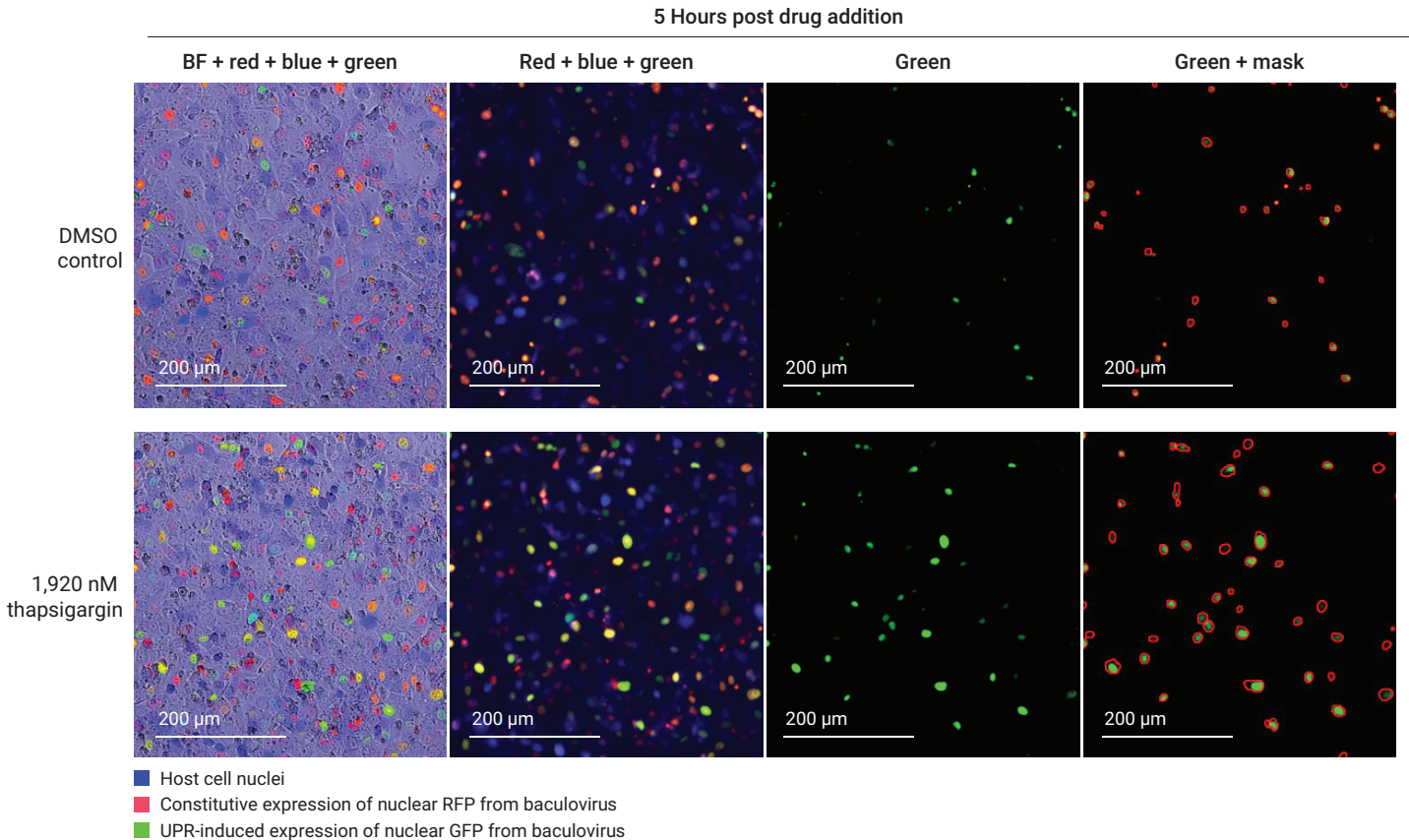

Figure 7. Fluorescent detection of UPR activation 5 hours post thapsigargin addition. Note about false coloring when red and green signals spatially overlap: if the green signal is more intense than the red signal the region is shown as green; if the red signal is more intense than the green signal, the region is shown as yellow. In the far right column eSight's mask, used to identify nuclei that contain GFP, is shown as a red outline.

Plotting the area under the GFP total integrated intensity curves as a function of thapsigargin concentration yields a canonical sigmoidal dose response curve (Figure 8C). The EC_{50} value (7.9 nM) determined from this image-based analysis compares very well with that determined using classical endpoint methods such as the inhibition of DNA synthesis (7 nM)[7], the inhibition of protein synthesis (5 nM)[7], and the inhibition of cell division (10 to 30 nM).[7]
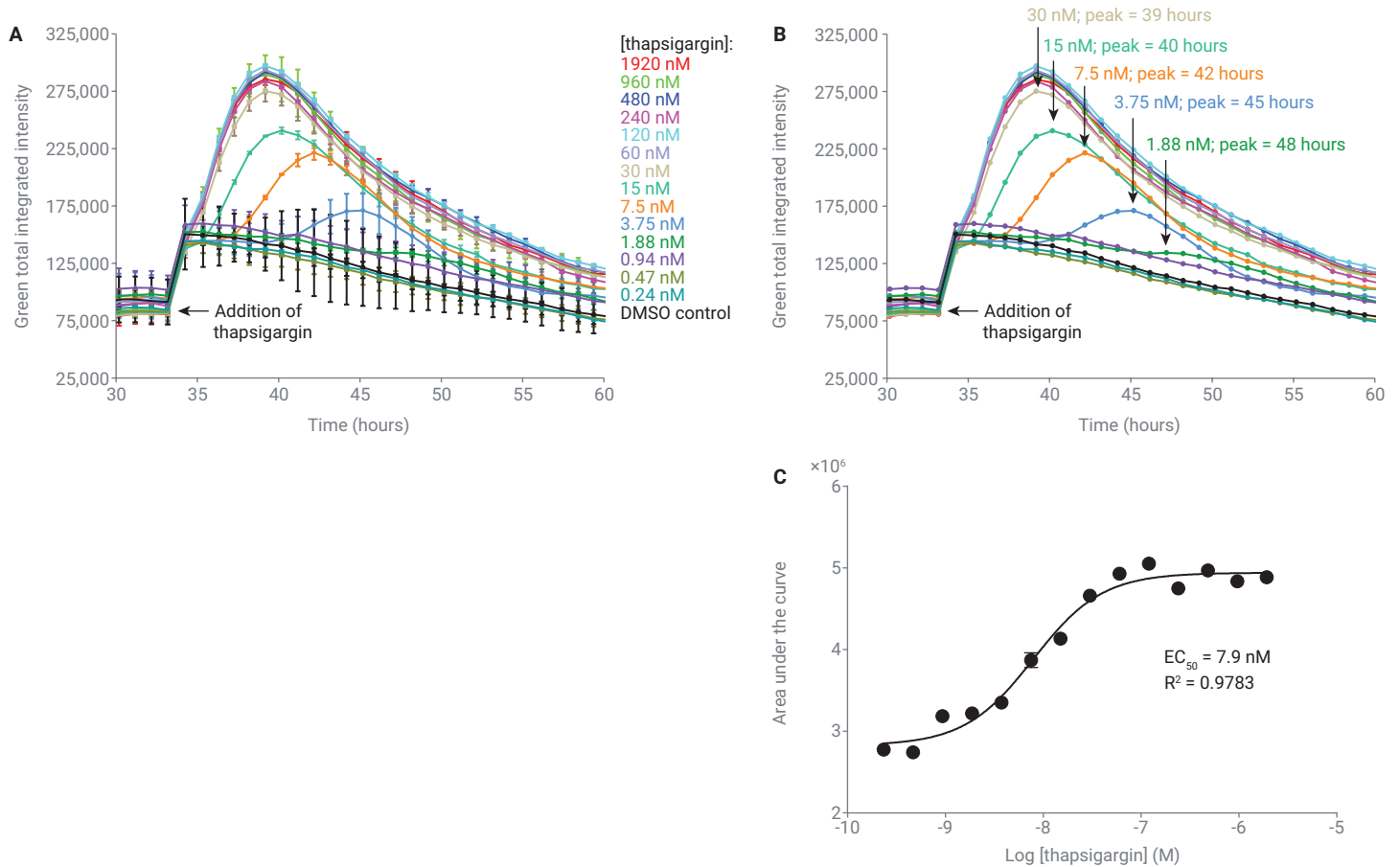

Figure 8. Real-time fluorescence-based quantification of thapsigargin-induced UPR activation. (A) Total integrated intensity of the GFP signal, produced by the UPR sensor, at different thapsigargin concentrations. Error bars reflect the standard deviation for two replicate wells. (B) The same data as panel "A", but with the error bars removed to highlight the dose-dependency of the curves. Black arrows highlight the time at which the GFP signal is maximal for five intermediate thapsigargin concentrations. (C) Dose response curve for thapsigargin titration, based on the area under the GFP total integrated intensity curves from panel "B".

Concurrent with its collection of live-cell images, eSight also tracked thapsigargin's impact on cell number/morphology/attachment strength using cellular impedance. Examining the DMSO negative control (black data trace) to establish a frame of reference, simply adding fresh media to the wells causes a transient spike in impedance that lasts roughly three hours; this is labeled as "phase 1" in Figure 9A. During the longer-lasting "phase 2" the impedance signal rises up until the ~43 hour time point, after which it gradually declines, which suggests that within the late time regime even the untreated cells are starting to lyse or attach to the plate bottom less tightly. Whereas low thapsigargin concentrations ≤1.88 nM have minimal impact on the cells' health/behavior, the intermediate concentrations of 3.75 and 7.5 nM actually cause the impedance traces to transiently increase above that of the DMSO control. This is a common response to intermediate concentrations of toxic compounds and will be discussed further in the Conclusion section. Thapsigargin concentrations from 15 to 1,920 nM cause a marked
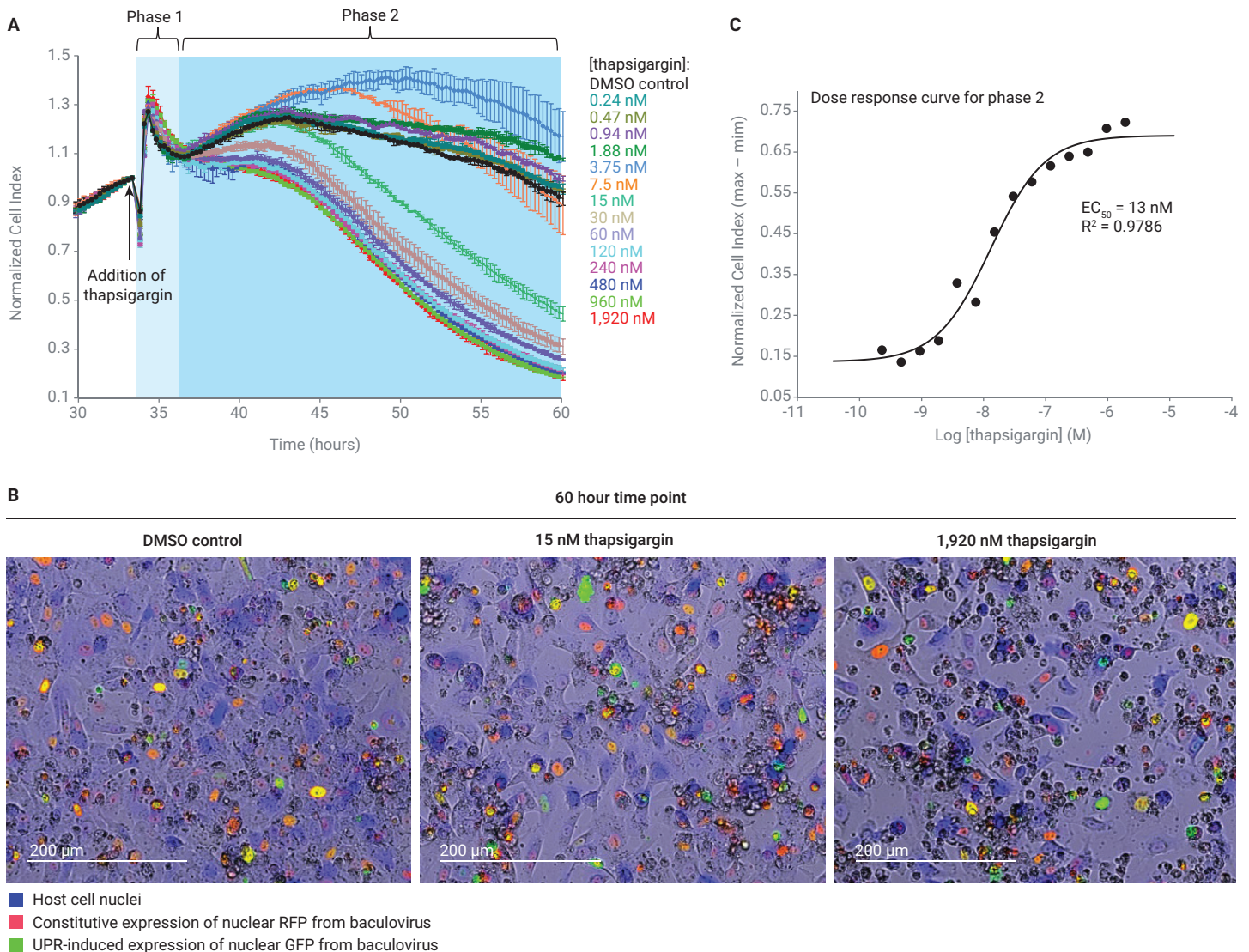
Figure 9. Real-time impedance-based quantification of thapsigargin-mediated cell killing. (A) Continuous readings of impedance at different thapsigargin concentrations. Note the rapid fluctuation during the first three hours post treatment (phase 1), followed by the slower sustained response (phase 2). Error bars reflect the standard deviation for two replicate wells. (B) Images from the 60 hour time point showing thapsigargin's cytotoxicity at different concentrations. See the legend for Figure 7 for notes about false coloring. Note that as cells die their fluorescent signals are largely lost. (C) Dose response curve for thapsigargin titration, based on the [max − min] parameter described in the text.

decrease in the impedance signal. This is consistent with cell shrinkage/lysis/detachment, which is confirmed by images from the 60 hour time point (Figure 9B).

Although an EC_{50} can be calculated from the impedance traces in phase 2 using a variety of methods, including area under the curves, the highest quality fitting was obtained by analyzing the difference between the maximum and minimum impedance values for each curve within the 36 to 60 hour time window. Plotting these "max−min" values as a function of the thapsigargin concentration yields the dose response curve in Figure 9C. Importantly, this EC_{50} value derived from impedance (13 nM) correlates extremely well with that derived from the image-based analysis of the fluorescent sensor (7.9 nM).

Conclusion

On their own, eSight's brightfield and impedance readouts are both clearly capable of detecting drug-mediated cytotoxicity (Figures 9B and 9A, repsectively). However, Montana Molecular's fluorescent UPR sensor takes what would otherwise be a generic cytotoxicity assay and transforms it into a highly specific tool for monitoring induction of the unfolded protein response in real time. The strong correlation between thapsigargin's EC_{50} as determined using the fluorescent UPR sensor (7.9 nM) versus using a traditional endpoint method (5 to 30 nM) validates the legitimacy of this approach for interrogating the UPR biochemical pathway in real time.

Figures 3, 4, 5, and 6 demonstrate, not surprisingly, that the utility of the UPR sensor varies dramatically depending on transduction/growth conditions. Although a lot of space in this application note is devoted to systematically comparing these different conditions, the entirety of that optimization data was

generated in a single assay involving just two 96-well plates. In contrast to endpoint assays where each well provides only a single data point, in the real-time eSight assay each well provides an entire time course and requires zero hands-on time once the assay has been initiated. This makes it possible to scan a broad array of conditions quickly and with ease. This process is also facilitated by the fact that the UPR sensor is dual color: since RFP expression is constitutive, the transcriptional accessibility of the baculovirus genome within the host cell nucleus can be evaluated without actually having to stimulate the UPR.

The image-based analysis parameter used here, GFP total integrated intensity, reflects both the number of cells that express GFP as well as the abundance of GFP in each cell. However, a wide variety of different analysis parameters are also available within the eSight software. The number of green cells/well, the average intensity of the green signal per cell, and the total green surface area in the well bottom were all evaluated (data not shown) and gave results similar to those presented above. Importantly, the dual color nature of the UPR sensor makes it possible to calculate the percentage of baculovirus containing cells that have UPR activated, or to generate ratiometric (GFP/RFP) plots. With so many output options available, it is important to employ the one that is most appropriate for the question being addressed.

When analyzing the data in Figure 9A it was noted that, similar to thapsigargin, other cytotoxic drugs have previously been found to cause a transient increase in the impedance signal when being used at intermediate concentrations; examples include A549 cells treated with MG132[8] and HeLa cells treated with doxorubicin. This may be a reflection of the cells being stressed and requiring a certain amount of time to overcome the stressor, whereas high concentrations

of the drug bypass this "coping phase" and instead funnel the cells directly into a death cascade. Because HT1080 cells do not form tight junctions, the transient increase in impedance caused by 3.75 and 7.5 nM thapsigargin cannot be attributed to changes in barrier function. Since these conditions do not cause changes in the number of cells that are present (data not shown), the only other explanations for the transient increase in impedance are changes in cell size or cell-substrate attachment strength. To probe these possibilities one would like to measure the size of the cells directly. Although eSight is capable of such a measurement, the format of the current assay does not allow for this. As seen in Figure 7, shortly after thapsigargin addition cells are packed together tightly – making it difficult to quantify their average surface area using brightfield. Since the ratio [nuclear volume/total cellular volume] is known to remain fairly constant[9] for diverse cell types, the average surface area of the red nuclei (i.e. only those containing the UPR sensor) was quantified as a surrogate for average cell size*. This value was found to be invariant throughout the course of the assay (data not shown). While this is consistent with thapsigargin not causing cells to expand and the transient impedance increase therefore being due to changes in cell-substrate adhsion strength, a much more rigorous analysis is warranted. The simplest next step would be to repeat the assay at much lower cell seeding density so that changes in the size of individual cells could be assessed directly.

* Focusing this analysis of average nuclear surface area on red nuclei has one disadvantage: If only a fraction of the red baculovirus-containing cells undergo UPR activation and concomitant swelling, the change in average red surface area will appear smaller than it actually is. However, quantifying changes in nuclear size using the other nuclear marker GFP, which would be specific to only those cells undergoing UPR activation, is not an acceptable alternative: As GFP accumulates, the amount of green surface area that is detectable increases, and this occurs whether nuclei are swelling or not.

The strong correlation between thapsigargin's EC_{50} based on imaging (7.9 nM) versus impedance (13 nM) is not surprising considering the fact that both readouts were obtained from the exact same population of cells over the same time period. If both readouts yield similar results, what is the benefit of employing both? One obvious benefit is that of obtaining a primary result and a confirmatory result via a single simple workflow. Another advantage of combining imaging

and impedance is that it provides an information richness that is not possible using either output alone. Imaging can provide highly specific information about cell health and behavior (in this case, UPR activation) that simply can not be deciphered directly from the impedance signal. On the other hand, because it is a composite readout that reflects changes in cell number/size/attachment strength/barrier function, impedance typically provides a sensitivity that is unmatched by imaging. As an

example of this, consider the overlooked "phase 1" of the impedance traces in Figure 9A. Zooming in on this phase, and subtracting out the background signal (DMSO control) reveals a legitimate dose dependency (Figure 10A) that is not detected by imaging. Because the concentration of DMSO was constant in all samples, the concentration-dependent fluctuations in impedance must be due to thapsigargin itself. Plotting the value of these impedance curves at the 34.6 hour time point as a function of
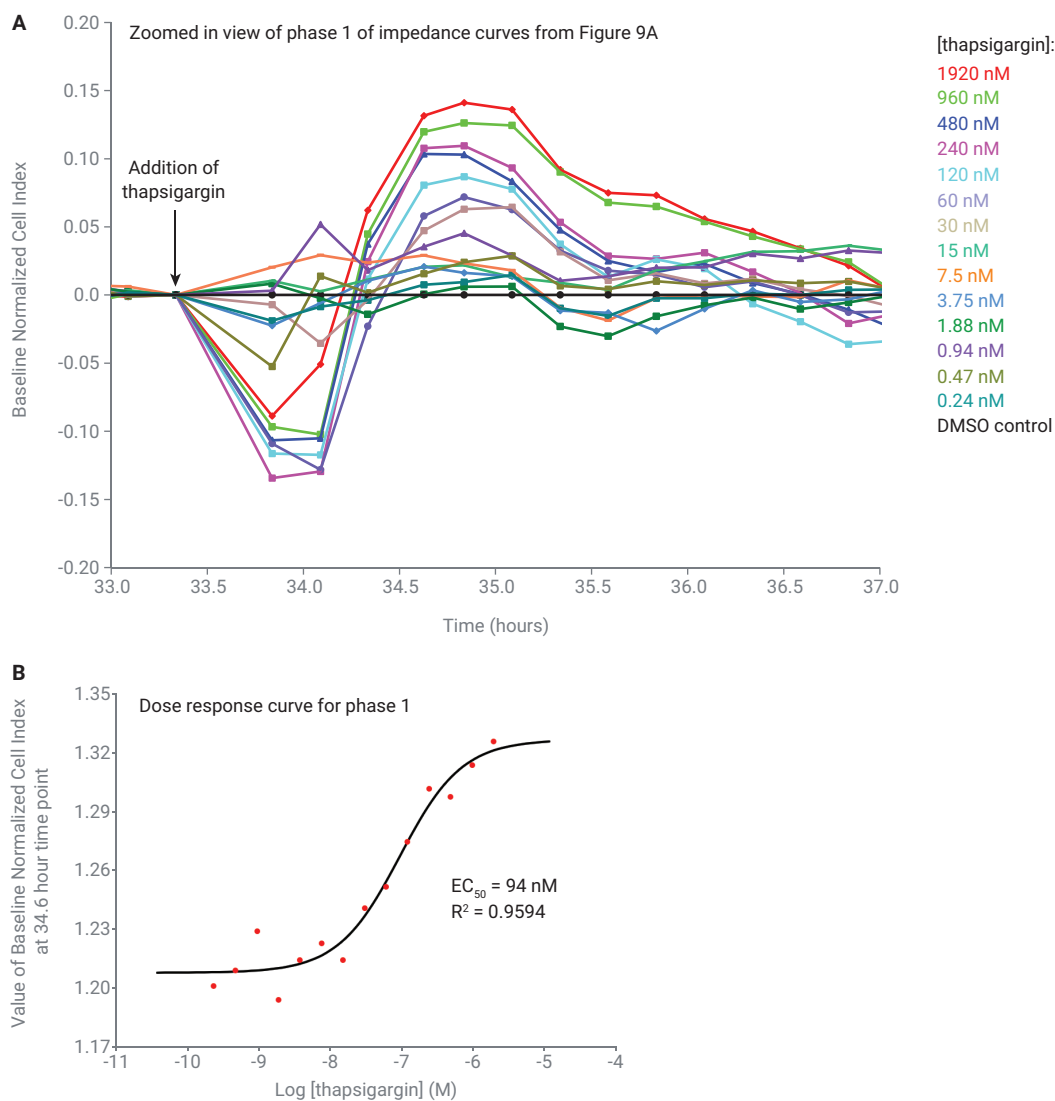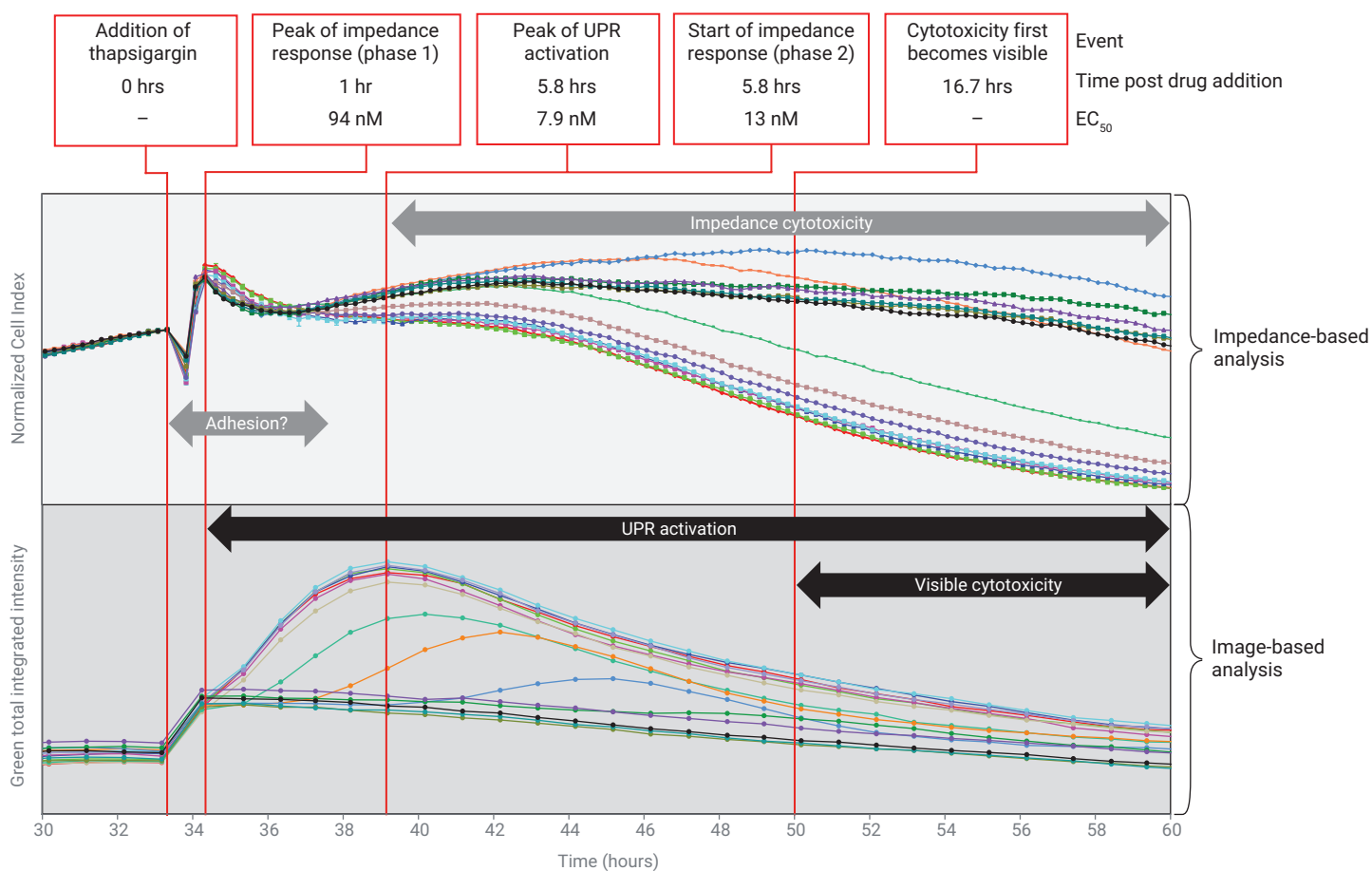

Figure 10. Real-time impedance-based quantification of thapsigargin-mediated cell killing. (A) Continuous readings of impedance at different thapsigargin concentrations. (B) Dose response curve for thapsigargin titration, based on the value of the curves from panel "A" at the 34.6 hour time point.

thapsigargin concentration yields the dose response curve in Figure 10B. This early, rapid phase of the impedance response most likely reflects biochemical phenomena distinct from the UPR because: i) it peaks ~4 hours prior to peak activation of the UPR, and ii) it has an EC_{50} (94 nM) that is substantially different than the EC_{50} determined from the UPR sensor (7.9 nM). For the same reasons described above, the impedance fluctuation in phase 1 can be attributed to neither changes in barrier function nor cell number. The fact that the average surface area of the red nuclei also does not change over this time frame suggests that phase 1

of the impedance response reflects the only remaining option: changes in cell-substrate attachment strength. This is quite reasonable considering thapsigargin's ability to rapidly increase cytosolic calcium concentrations[10] and the multiple roles that calcium plays in modulating cellular adhsion. Although additional experiments would be required to confirm this, the key point from Figure 10 is that without impedance one would never know that this rapid and transient effect of thapsigargin existed.

If one wishes simply to identify UPR activating compounds within a library, or to quantitatively characterize the efficacy of library hits, the eSight assay presented

here is more than capable of filling these roles. On the other hand, if the goal is to extract as much information as possible about a compound's effect, including but not limited to UPR, eSight also meets this need by simultaneously using two unique analytical methods to provide a staggering amount of relevant information from a single, simple assay (Figure 11). In instances where eSight's dual output does not immediately provide mechanistic insight, simply repeating the assay under different conditions (such as lowering the cell density, as described above) is often all that is necessary for providing clarity.

Addition of thapsigargin	Peak of impedance response (phase 1)	Peak of UPR activation	Start of impedance response (phase 2)	Cytotoxicity first becomes visible	Event
0 hrs	1 hr	5.8 hrs	5.8 hrs	16.7 hrs	Time post drug addition
–	94 nM	7.9 nM	13 nM	–	EC_{50}

Figure 11. Summary of kinetic information derived from eSight's impedance- and image-based readouts. Red lines denote the timing of key events. Visible cytotoxicity, not discussed in the text, first became apparent at the ~50 hour time point.

Acknowledgment

References

1. Hetz, C. *et al.* Mechanisms, Regulation and Functions of the Unfolded Protein Response. *Nat. Rev. Mol. Cell. Biol.* **2020**, *21(8)*, 421.

2. Adams, C. J. *et al.* Structure and Molecular Mechanism of ER Stress Signaling by the Unfolded Protein Response Signal Activator IRE1. *Front. Mol. Biosci.* **2019**, Mar 12, *6*, 11.

3. Wei, S. *et al.* Baculovirus IE2 Interacts with Viral DNA Through Daxx to Generate an Organized Nuclear Body Structure for Gene Activation in Vero Cells. *J. Virol.* **2019**, *93(8)*, e00149-19.

4. Fujita, R. *et al.* An HDAC Inhibitor Increases AcMNPV Gene Expression in Mammalian Cells. *Arch. Virol.* **2010**, *155(4)*, 577.

5. Thastrup, O. *et al.* Thapsigargin, a Tumor Promoter, Discharges Intracellular Ca2+ Stores by Specific Inhibition of the Endoplasmic Reticulum Ca2(+)-ATPase. *PNAS* **1990**, *87(7)*, 2466.

6. Sehgal, P. Inhibition of the Sarco/Endoplasmic Reticulum (ER) Ca2+-ATPase by Thapsigargin Analogs Induces Cell Death Via ER Ca2+ Depletion and the Unfolded Protein Response. *J. Biol. Chem.* **2017**, *292(48)*, 19656.

7. Gosh, T. K. *et al.* Persistent Intracellular Calcium Pool Depletion by Thapsigargin and its Influence on Cell Growth. *J. Biol. Chem.* **1991**, *266(36)*, 24690.

8. Zhang, J. *et al.* Combining Live-cell Imaging with Cellular Impedance to Monitor Apoptotic Cell Death in Real Time. https://www.agilent.com/cs/library/applications/application-combining-live-cell-imaging-cell-analysis-5994-1212en-agilent.pdf

9. Cantwell, H. *et al.* Unravelling Nuclear Size Control. *Curr. Genet.* **2019**, *65(6)*, 1281.

10. Jones, K. T. *et al.* Thapsigargin Raises Intracellular Free Calcium Levels in Human Keratinocytes and Inhibits the Coordinated Expression of Differentiation Markers. *Exp. Cell Res.* **1994**, *210(1)*, 71.

www.agilent.com/chem

Agilent

Trusted Answers